Brain circuitries in control of feeding behaviors

Focus on Neuropeptide Y

Gumbs, M.C.R.

Chapter V.
Neuropeptide Y activity in the nucleus accumbens modulates feeding behavior and neuronal activity

van den Heuvel, J.K., Gumbs, M.C.R.*, Furman, .K*, Eggels, L., Opland, D.M., Land, B.B., Kolk, S.M., Narayanan, N., Fliers, F., Kalsbeek, A., DiLeone, R.J., and la Fleur, S.E.
Biological Psychiatry, 77(7):633-641 (2015)
*These authors contributed equally to the manuscript

Abstract

Neuropeptide Y (NPY) is a hypothalamic neuropeptide that plays a prominent role in feeding and energy homeostasis. Expression of the NPY receptor subtype 1 (NPY1R) is highly concentrated in the nucleus accumbens (NAc), a region important in the regulation of palatable feeding. In this study, we performed a number of experiments to investigate the actions of NPY in the NAc. First, we determined caloric intake and food choice after bilateral administration of NPY in the NAc in rats on a free-choice diet of saturated fat, a 30% sucrose solution, and standard chow (fcHFHS), and whether this was mediated by the NPY1R. Second, we measured the effect of intra-NAc NPY on neuronal activity using *in vivo* electrophysiology. Third, we examined co-localization of NPY1R with enkephalin and dynorphin neurons, and the effect of NPY on *preproenkephalin* (*ppENK*) mRNA levels in the striatum using fluorescent and radioactive *in situ* hybridization. Finally, using retrograde tracing, we examined whether NPY neurons in the arcuate nucleus (Arc) of the hypothalamus project to the NAc.

In rats on the fcHFHS diet, intra-NAc NPY increased intake of fat, but not of the sucrose solution or chow, and this was mediated by the NPY1R. Intra-NAc NPY reduced neuronal firing, as well as *ppENK* mRNA expression in the striatum. Moreover, NAc enkephalin neurons expressed *Npy1r* and Arc NPY neurons project to the NAc.

We conclude that NPY reduces neuronal firing in the NAc, resulting in increased palatable food intake. Together, our neuroanatomical, pharmacological, and neuronal activity data support a role and mechanism for intra-NAc NPY-induced fat intake.

Introduction

A major population of Neuropeptide Y (NPY)-producing neurons is located in the arcuate nucleus (Arc) of the hypothalamus. Central administration of NPY increases feeding behavior in rodents (Clark et al., 1984; Levine & Morley, 1984; Stanley & Leibowitz, 1984), and NPY has been linked to the control of carbohydrate intake (Stanley, Daniel, et al., 1985; van den Heuvel, Eggels, van Rozen, et al., 2014). However, we recently observed that when NPY is administered in the lateral ventricle of rats on a free-choice high-fat high-sugar (fcHFHS) diet, it was not sugar, but rather saturated fat and chow consumption that increased (Stanley, Chin, et al., 1985). The link between NPY and carbohydrate intake has been previously studied using administration of NPY into specific hypothalamic regions (Stanley, Chin, et al., 1985; Stanley, Daniel, et al., 1985). In contrast, we administered NPY into the lateral ventricle, providing contact with not only the hypothalamus, but also with corticolimbic areas involved in reward and motivation, such as the nucleus accumbens (NAc) where NPY receptors are localized (Kishi et al., 2005; Pickel et al., 1998; Wolak et al., 2003). It remains to be explored, however, whether direct action of NPY in the NAc regulates fat consumption.

Reduced neuronal activity in the NAc occurs during feeding and intra-NAc administration of orexigenic compounds, such as melanin concentrating hormone and muscimol, inhibit NAc neuronal activity (Basso & Kelley, 1999; Krause et al., 2010; Sears et al., 2010; Stratford & Kelley, 1997). However, it is not known whether NPY also affects neuronal activity in the NAc. Given that direct NPY administration into other brain areas, including the amygdala and Arc, reduces neuronal activity (Acuna-Goycolea et al., 2005; Giesbrecht, Mackay, Silveira, Urban, & Colmers, 2010), we hypothesized that NPY reduces NAc neuronal activity and that this is associated with increased fat intake.

Opioids have an established role in reward behavior, and opioid-expressing neurons are located within the NAc. Of the opioid-expressing neurons, enkephalin neurons are of specific interest as they express dopamine D2 receptors (DRD_2) and have been linked to high-fat feeding; i.e. NAc enkephalin gene expression is affected by consumption of the highly palatable Ensure drink (Kelley et al., 2003), which contains fat and sugar, and striatal DRD_2 availability is correlated with high-fat intake (van de Giessen et al., 2013). Moreover, enkephalin binds to mu-opioid receptors and local NAc administration of the mu-opioid receptor agonist DAMGO specifically increases intake of high-fat foods (M. Zhang et al., 1998). In turn, the DAMGO-induced increased intake of high-fat foods is NPY receptor subtype 1 (NPY1R) dependent (H. Zheng et al., 2010). Therefore, the effect of NPY on fat intake may involve changes in NAc enkephalin levels. Given these findings, we hypothesized that NPY1Rs are localized on enkephalin neurons and that intra-NAc NPY injection alters striatal enkephalin levels.

Finally, previous studies have revealed anatomic connections between the Arc and NAc (Brog, Salyapongse, Deutch, & Zahm, 1993; Yi et al., 2006) as well as the presence of NPY

receptors in the NAc (Kishi et al., 2005; Pickel et al., 1998; Wolak et al., 2003). While a recent study found α-MSH projections from the Arc to NAc (Lim, Huang, Grueter, Rothwell, & Malenka, 2012), it has not been determined whether NPY neurons in the Arc project to the NAc.

To examine the action of NPY in the NAc we first assessed food intake and *preproenkephalin* (*ppENK*) mRNA responses to intra-NAc NPY injections in rats on the fcHFHS diet. Second, we measured NPY's effects on neuronal activity using *in vivo* electrophysiology. Third, using fluorescent imaging and retrograde tracing we determined whether NPY1Rs are localized on enkephalin and dynorphin neurons and whether NPY neurons in the Arc project to the NAc. We found that intra-NAc NPY stimulates fat intake via the NPY1R and is associated with reduced expression of *ppENK* mRNA and neuronal activity. Moreover, enkephalin neurons express NPY1Rs and NPY neurons in the Arc project to the NAc. These neuroanatomical, pharmacological, and neuronal activity data support a possible role and mechanism for intra-NAc NPY-induced fat intake.

Experimental Procedures

Animals

For behavior and radioactive *in situ* hybridization, male adult Wistar rats (Charles River, Germany) weighing 270-300 g were used. For electrophysiological experiments and fluorescent *in situ* hybridization, C57/BL6 mice (Jackson Labs, Bar Harbor, Maine, USA) weighing 25-30 g were used. All animal procedures were performed in accordance with the protocol approved by the Yale Institutional Animal Care and Use Committee, and the Committee for Animal Experimentation of the Academic Medical Center of the University of Amsterdam.

Effect of intra-accumbens NPY and NPY1R antagonist on food intake

Rats were housed in a temperature- (21-23 °C) and light-controlled room (lights on 7:00–19:00). One week after arrival, rats were implanted with two cannulas aimed bilaterally at the NAc-shell as described in the Supplemental Materials. One week after surgery, rats (N = 15) were placed on a free-choice high-fat high-sugar (fcHFHS) diet and were able to choose from the following components: a dish of saturated fat (Beef tallow (Ossewit/Blanc de Boeuf), Vandemoortele, Belgium), a bottle of 30% sugar water (mixed from commercial grade sugar and tap water), standard chow (special diet service [SDS], England) and a bottle of tap water.

After 1 week of fcHFHS diet exposure, 0.6 µg NPY (minimum effective dose in previous experiments (C. M. Brown et al., 2000; C. M. Brown, Fletcher & Coscina, 1998; own observations) or vehicle (1x phosphate buffered saline [PBS]) was administered at the beginning of the light phase (between 10:00 and 11:00) in a balanced design. NPY was

obtained from Bachem, Germany (H6375), and dissolved in 1xPBS. Before the start of the experiment, all food components (except water) were removed from the cage. 33-gauge injector cannula's (Plastics One, Bilaney Consultants GmbH, Düsseldorf, Germany), extending 1 mm below the guide cannula, were inserted into the guide cannula's, and animals received bilateral infusions of 0.3 µL fluid per site at a rate of 0.15 µl/min via a syringe infusion pump. Injections were confirmed by monitoring fluid movement in the tubing via a small air bubble. After completion of the injection, the injector was left in place for 1 min to allow for diffusion. Upon completion of all infusions, food was returned to the cages and all individual food components were measured after 2, 5 and 24 hours, and caloric intake (kcal) for each individual food item and total caloric intake were calculated. Total caloric intake was defined as the sum of each individual food component for which the caloric density was defined as follows, chow: 3.31 kcal/g; fat: 9 kcal/g and sucrose solution: 1.2 kcal/g. The experiment was repeated 3 days later according to a cross-over design.

At the end of the experiment, food was removed in the morning (and not returned) and rats received intra-NAc injection of vehicle or 0.6 µg NPY. One hour later, rats were anesthetized and transcardially perfused with ice-cold saline followed by 4 % paraformaldehyde, and brains were post-fixed for 24 hours. Brains were washed in PBS, cryoprotected in 30 % sucrose at 4 ^{o}C, and subsequently frozen on dry ice and stored at -80 ^{o}C. Cryostat sections were cut at 35 µm and mounted on Superfrost Plus slides (Fisher, Gerhard Menzel GmbH, Germany). Some slides were stained for Nissl with thionine, and checked for cannula placement with inclusion criteria described below. Remaining slides were air-dried and stored at -80 ^{o}C to be used for radioactive *in situ* hybridization. The procedure for radioactive *in situ* hybridization was performed as described previously (van den Heuvel, Eggels, Fliers, et al., 2014) and described in the Supplemental Materials.

In a separate experiment, we tested whether the NAc NPY1R is involved in the intra-NAc NPY-induced increased fat intake by intra-NAc administration of the NPY1R antagonist GR231118 (synonym of LY1229U91, Sigma Aldrich, Zwijndrecht, the Netherlands) or vehicle in a volume of 0.2 µl in the NAc, 15 min before intra-NAc NPY in rats on the fcHFHS diet (N = 15). These experiments were conducted according to the same protocol (for surgery and cannula placement verification) as described above. We only measured intake of chow, fat and sugar water at one time point as NPY effects do not show beyond a few hours. The dose of antagonist used (0.3 µg) was chosen based on reports published elsewhere (Faulconbridge, Grill, & Kaplan, 2005; Skibicka, Shirazi, Hansson, & Dickson, 2012), and on a dose response in a few animals using 0.3, 1 and 3 µg antagonist (see appendix). Since 1 and 3 µg in the NAc decreased overall intake, we choose the 0.3 µg dose, because it did not significantly affect feeding behavior (data not shown). At the end of the experiment, rats were killed by decapitation and brains were removed, frozen on dry ice and stored at -80 ^{o}C. Cryostat sections were stained for Nissl with thionine and checked for cannula placement. Data of rats

were only included when we verified that they had unilateral or bilateral cannula placement in the NAc-shell between Bregma 1.0 and 2.20 mm (Paxinos & Watson, 2007; Pecina & Berridge, 2000; Reynolds & Berridge, 2001). Based on these criteria, 5 animals were excluded from analysis from experiment 1, and 1 animal from experiment 2 (with NPY1R antagonist). Furthermore, for experiment 2, data from 3 more animals were excluded from analysis due to loss of the cannula or sickness behavior after injection, which turned out to be associated with infection around the cannula.

Fluorescent *in situ* hybridization

Fluorescent *in situ* hybridization was performed as described previously (Georgescu et al., 2005), and in the Supplemental Materials. Probes for double *in situ* hybridization were prepared using an *in vitro* transcription kit with digoxigenin-labeled UTP (Roche, Basel, Switzerland) for making the *Npy1r* probe, or fluorescein-labeled UTP (Molecular Probes, Eugene, OR, USA) for making the *ppENK* or *prodynorphin* probe (information on probes is provided in the Supplemental Materials).

In vivo electrophysiology

Four well-habituated C57/BL6 mice (25-30 g) were implanted with a cannula (Plastics One) and arrays of microwire electrodes (Tucker-Davis Technologies, Alachua, FL, USA) using aseptic stereotactic methods described in detail previously (Sears et al., 2010), and in the Supplemental Materials. The arrays consisted of 16 Teflon-coated, 50 µm stainless steel wires arranged in an 8×2 configuration, with each electrode spaced by ~250 µm. The *in vitro* impedance of the electrodes was 100–300 kΩ. After a recovery period of 5-7 days, animals were acclimatized to recording procedures (i.e. headsets and cables were attached to the implants) for 1 day. Drug infusions were performed as follows. Animals were lightly anesthetized with halothane via a nosecone during the experiment, and recording head stages were plugged in. After initial recording, data acquisition was paused and animals were infused with either aCSF (NaCl 147 mM, $CaCl_2$ 1.3 mM, $MgCl_2$ 0.9 mM, KCl 4.0 mM) or NPY (0.6 µg). Infusions were made through 33-gauge cannula (Plastics One) that protruded 0.2 mm from the tip of the guide cannulas. Injectors were inserted into the guide cannulas and 0.3 µL of infusion fluid was delivered per site at a rate of 0.15 µl/min via a syringe infusion pump (KDS Scientific, Holliston, MA, USA). Fluid was infused via 0.38 mm-diameter polyethylene tubing that connected the injector to a 5 µL Hamilton syringe. Injections were confirmed by monitoring movement of fluid in the tubing via a small air bubble. After injection was complete, the injector was left in place for 2 min to allow for diffusion. Infusions took place between 12:00 and 14:00. Recording data were collected for 1 hour after infusions.

Neuronal ensemble recordings were made using a Many Neuron Acquisition Program (Tucker-Davis Technologies). Putative single neuron units were identified on-line using an oscilloscope and an audio monitor. The Tucker-Davis Technologies off-line sorter was used to analyze the signals off-line and to remove artifacts due to cable noise and behavioral devices (pump, click stimulus). Principal component analysis (PCA) and waveform shape were used for spike sorting. Single units were identified as having (1) consistent waveform shape, (2) separable clusters in PCA space, (3) average amplitude estimated at least three times larger than background activity, and (4) a consistent refractory period of at least 2 ms in interspike interval histograms. Units identified on-line as potential single units that did not meet these criteria off-line were not included in this analysis. Datasets were previewed using OpenSorter (Tucker-Davis Technologies), and subsequently analyzed using custom routines for MATLAB. For each well-isolated neuron, post-infusion firing rates were normalized to mean pre-infusion firing rates (in the 10 min immediately preceding drug infusion) and binned (60-second bins). Activity was then compared between neurons recorded in NPY and aCSF conditions.

At the end of the experiment, mice were perfused transcardially with ice-cold saline followed by 4 % paraformaldehyde. After fixation, brains were cryoprotected in 30 % sucrose at 4 ^{o}C overnight. Microtome sections were cut at 40 µm along the horizontal axis and mounted on Superfrost Plus slides (Fisher). Electrode and cannula placement was verified microscopically in horizontal sections using the mouse brain atlas from Paxinos and Franklin (2004).

CTB tracing

One week after arrival, 6 male Wistar rats (Charles River; Sulzfeld, Germany) weighing 270-300 g were implanted two cannula's: one aimed at the right NAc shell for infusion of the cholera toxin B (CTB) conjugated to Alexa-555 (C-22843, Invitrogen, Bleiswijk, the Netherlands) tracer and one cannula in the left lateral ventricle (LV) for the infusion of colchicine to block neuronal transport (C9754, Sigma-Aldrich, Zwijndrecht, the Netherlands).
Surgical procedures were the same as for the rat study described above. For the LV, a permanent 22-gauge stainless steel guide cannula was used with coordinates 0.8 mm posterior from Bregma, 1.4 mm lateral from midline, and 4.5 mm below the surface of the brain. In contrast to CTB, fluorophore-labeled CTB cannot be applied by iontophoresis, so we used pressure injection (Yi et al., 2006). Rats were injected unilaterally with 100 – 150 nl 1% CTB into the NAc shell. The injection needle was left in place and fixed with dental cement to the skull to minimize leakage from the tract (Yi et al., 2006). Twelve days later, rats were deeply anesthetized and 100 µg colchicine in 5 µL PBS was injected into the lateral ventricle. 24-36 hours later, rats were transcardially perfused with saline, followed by a solution of 4 % paraformaldehyde in 0.1 M PBS (pH 7.4) at 4 ^{o}C. Brains were removed and kept in a 30 %

sucrose solution dissolved in PBS. Subsequently, the brains were washed briefly with PBS, frozen on dry ice and stored at -80 ^{o}C until further processing for fluorescent immunohistochemistry. The procedures for fluorescent immunohistochemistry were performed as described previously (Kolk, Whitman, Yun, Shete, & Donoghue, 2006) and in the Supplemental Materials.

Statistical analyses

For the effects of NPY on food intake and on *enkephalin* mRNA, t-tests were performed. The data on NPY in combination with the NPY1R antagonist were tested with a Two-way repeated measures ANOVA (for paired-comparison), and were followed with Sidak's multiple comparisons tests. Data obtained with electrophysiology were analyzed with a repeated-measures ANOVA, followed by Tukey's *post hoc* tests where appropriate. For all analyses, significance was assigned at the $p \leq 0.05$ level. All data are presented as mean ± SEM.

Results

Effect of NPY and NPY1R antagonist in nucleus accumbens on food intake

Local administration of NPY significantly increased fat intake after 2 hours (Figure 1A), but not after 5 or 24 hours (Supplemental Data S1). Intra-NAc NPY did not affect intake of the chow or sugar component after 2 hours (Figure 1A), or after 5 or 24 hours (Supplemental Data S1).
Subsequently, the effect of pretreatment with the selective NPY1R antagonist GR231118 on NPY-induced fat intake was tested. Again, when infused in the NAc, NPY specifically increased fat intake (Supplemental Data S2). Interestingly, when cannula's were placed bilaterally in the shell of the NAc (which was the case in 5 out of 11 animals), pretreatment with NPY1R antagonist completely prevented the NPY-induced increase in fat intake (*Interaction* effect for Pretreatment with NPY1-antagonist*NPY ($F_{1,20} = 6.3$; $p = 0.02$); a trend for an NPY effect: $F_{1,20} = 3.5$; $p = 0.08$), and no effect of the NPY1 antagonist $F_{1,20} = 1.5$; $p = 0.24$; see Figure 1B).

NPY reduces cell firing in the nucleus accumbens *in vivo*

To evaluate the effects of NPY on neuronal activity *in vivo*, neuronal firing data were collected during intra-NAc infusions of aCSF or NPY with microwire recording electrodes implanted in the NAc (Figures 2A-B). Multi-unit recordings performed under anesthesia revealed a significant reduction in firing rates of NAc neurons treated with 0.6 μg NPY (N = 29) and a significant *Interaction* between Time and Treatment (Two-way ANOVA $F_{39,1482} = 1.874$, $p = 0.0010$; Figures 2C-D). Firing in 11/29 (37.9 %) units was suppressed 50 % below baseline. Another 9/29 (31.0 %) units were suppressed 25 % below baseline. The remaining 9 units were either unchanged (6/29, 20.7 %) or increased (3/29, 10.3 %) relative to pre-infusion firing rates. This effect lasted 25 min, starting within 5 min after infusion (Figure 2C).

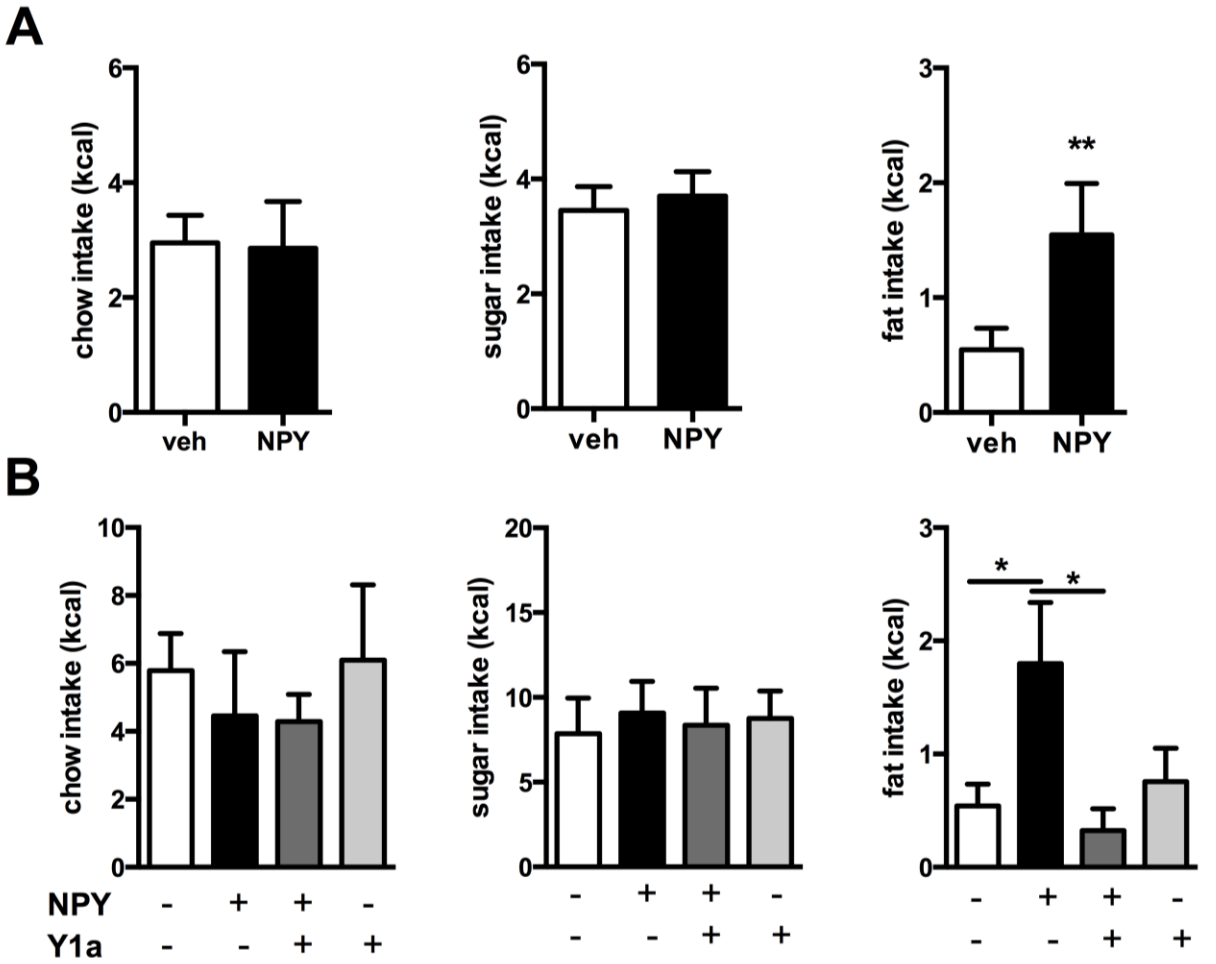

Figure 1. Effects of intra-NAc NPY in rats on intake of chow, sugar, and fat components of the fcHFHS diet. A) NPY in the NAc significantly increased fat intake and not sugar or chow intake; total intake tended to be increased (veh 6.5 ± 0.8 *vs.* NPY 8.7 ± 1.1; p = 0.1; N = 10). **B)** The increase in fat intake was prevented by pretreatment with the NPY1R antagonist GR231118 (Y1a) injected bilaterally into the shell of the NAc, whereas the NPY1R antagonist did not affect fat intake (or chow and sugar intake) alone (N = 5). A significant effect is depicted by *p < 0.05 and **p < 0.01. Data are presented as mean ± *SEM.*

Npy1r co-localizes with enkephalin- and dynorphin-positive neurons in the nucleus accumbens

Since NPY receptors are present in the NAc (Kishi et al., 2005), we investigated whether *Npy1r* co-localizes with enkephalin and dynorphin neurons by performing double-labeled fluorescent *in situ* hybridization. Co-localization of *Npy1r* on enkephalin and dynorphin neurons was found throughout the striatum and NAc; about 59 % of *Npy1r* co-localized with enkephalin neurons (Figure 3A), and about 18 % with dynorphin neurons (Supplemental Data S3) as revealed by confocal analysis.

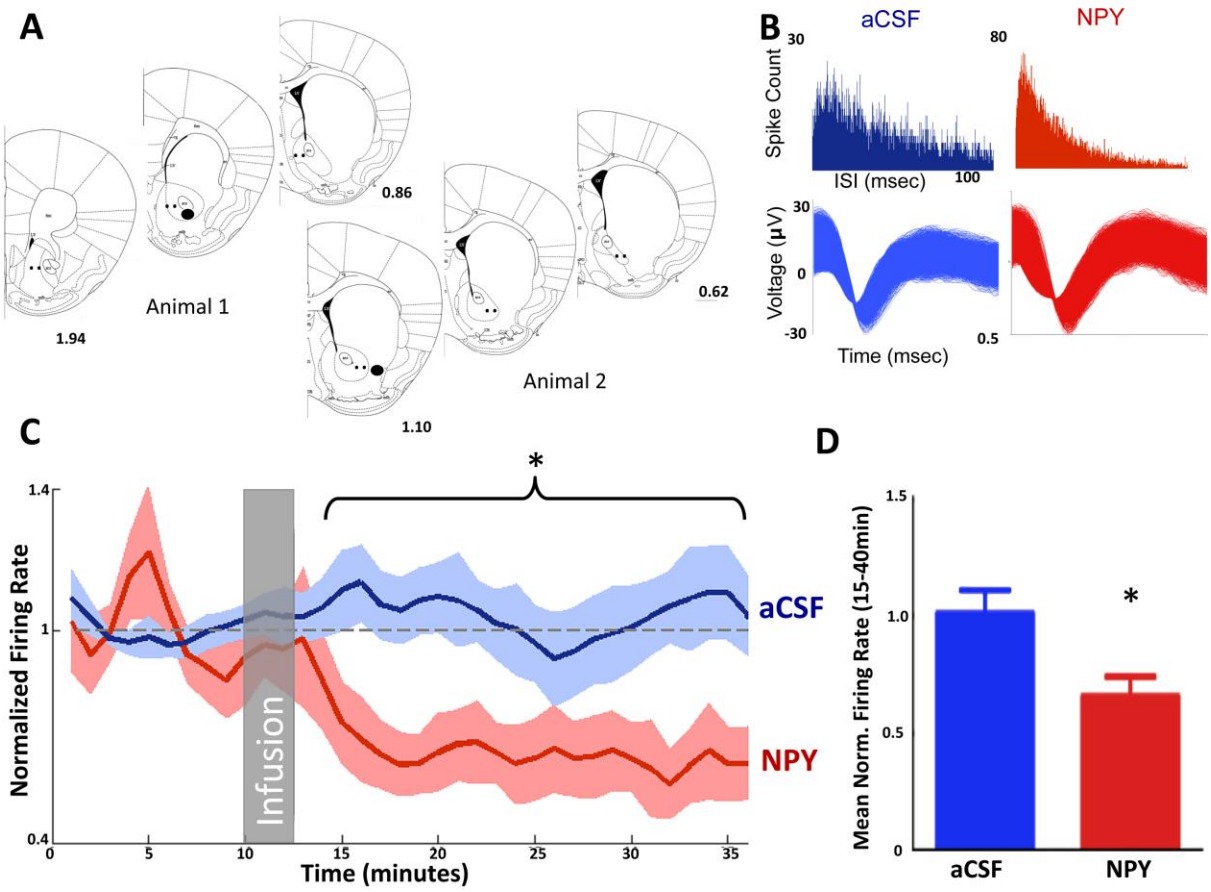

Figure 2. NPY in the NAc decreases neuronal activity *in vivo*. A) Location of electrodes (black spots) and cannula's (filled black circles) projected on an mouse brain atlas section (Paxinos & Franklin, 2004). **B)** Interspike interval histograms and waveforms from a single unit in aCSF infusion sessions (left) and the same neuron in NPY infusion sessions (right). **C,D)** Average neuronal activity for NPY sessions and aCSF. Gray box represents time of infusion. NPY significantly reduces firing rate from 15-40 min. *$p < 0.05$, aCSF = artificial cerebrospinal fluid.

NPY administration in the nucleus accumbens decreases *ppENK* mRNA expression

Striatal enkephalin, as opposed to dynorphin, has been described to be affected by changes in energy balance (Will, Vanderheyden, & Kelley, 2007). Additionally, we found that *Npy1r* is mainly located on enkephalin neurons. Therefore, we investigated the effect of NPY on *enkephalin* mRNA levels. We quantitatively measured *ppENK* mRNA levels using radioactive *in situ* hybridization and found that one hour after intra-NAc NPY administration, *ppENK* mRNA expression was significantly downregulated in both the ventral striatum (NAc) as well as the dorsal striatum (Figure 3B; $p < 0.05$).

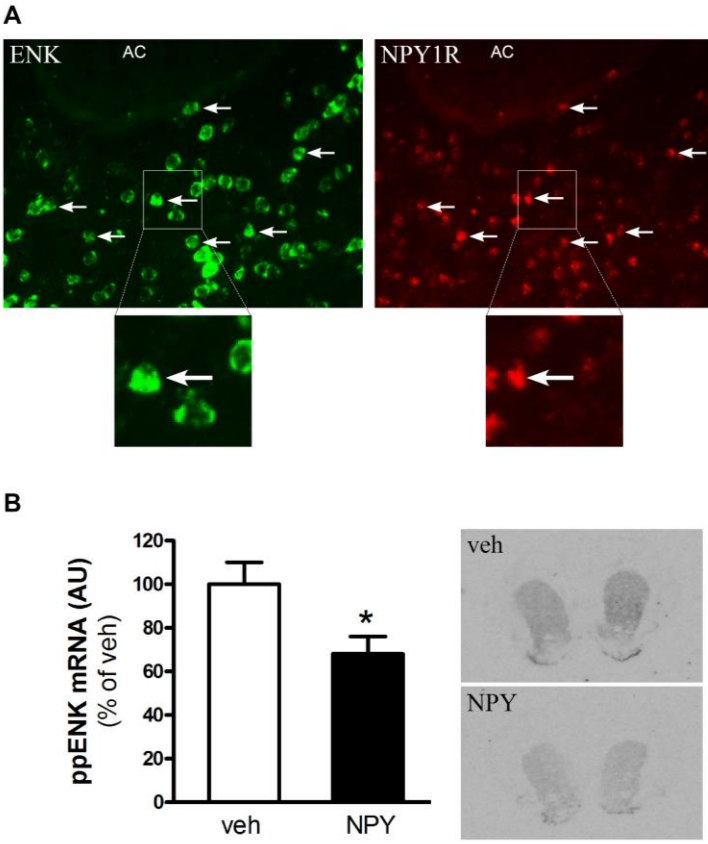

Figure 3. The NPY1 receptor (NPY1R) is expressed on enkephalin (ENK) neurons in the nucleus accumbens (NAc) and intra-NAc NPY downregulates *ppENK* mRNA levels. A) Expression patterns of *Npy1r* and *ppENK* in the NAc. Horizontal arrows indicate co-localization. **B)** *ppENK* gene expression levels in the ventral striatum and representative images after intra-NAc injection of NPY. Values are mean ± *SEM* of seven to nine rats per group. *p < 0.05 NPY *vs.* vehicle, AC = anterior commissure.

A subset of arcuate nucleus NPY neurons projects to the nucleus accumbens

To investigate the origin of NPY neurons projecting to the NAc, the CTB tracer was administered in the NAc and co-localization with NPY antibody was determined. The tracer was mostly concentrated at the border of the medial shell and core, positioned dorsomedial to the anterior commissure (AC; Figure 4A). Anterograde CTB tracing was found in the medial part of the subcommissural ventral pallidum and lateral hypothalamus confirming previous findings (Christie, Summers, Stephenson, Cook, & Beart, 1987; Heimer, Zahm, Churchill, Kalivas, & Wohltmann, 1991; Kirouac & Ganguly, 1995). In this study, our main focus was to investigate afferent projections to the NAc and consequently to determine which of these projections co-label with NPY. Retrograde transport of CTB tracer was examined by serial sectioning and immunostaining in the neocortex, thalamus, hypothalamus, amygdaloid nuclei, ventral pallidum and subiculum.

Consistent with previous studies, CTB staining was found in labelled perikarya in the agranular insular cortex, perirhinal cortex, midline thalamic nuclei and (baso)lateral amygdala (Brog et al., 1993; Christie et al., 1987; Kirouac & Ganguly, 1995). However, in none of these areas did CTB co-localize with NPY staining.

The primary site for synthesis of NPY peptide is the Arc. Consistent with others (Brog et al., 1993; Yi et al., 2006), we found CTB staining in the Arc. CTB labeling was present in the ventromedial and ventrolateral part the Arc. In the ventromedial Arc, the majority of CTB cells were dually immunostained with NPY (Figure 4B), indicating NPY-positive cells projecting from the Arc to NAc. This finding was confirmed in 3 successfully injected cases. CTB cells in the lateral portion of the Arc, which did not co-localize with NPY, may be α-MSH neurons as melanocortinergic projections from the Arc to NAc have been shown previously (Lim et al., 2012).

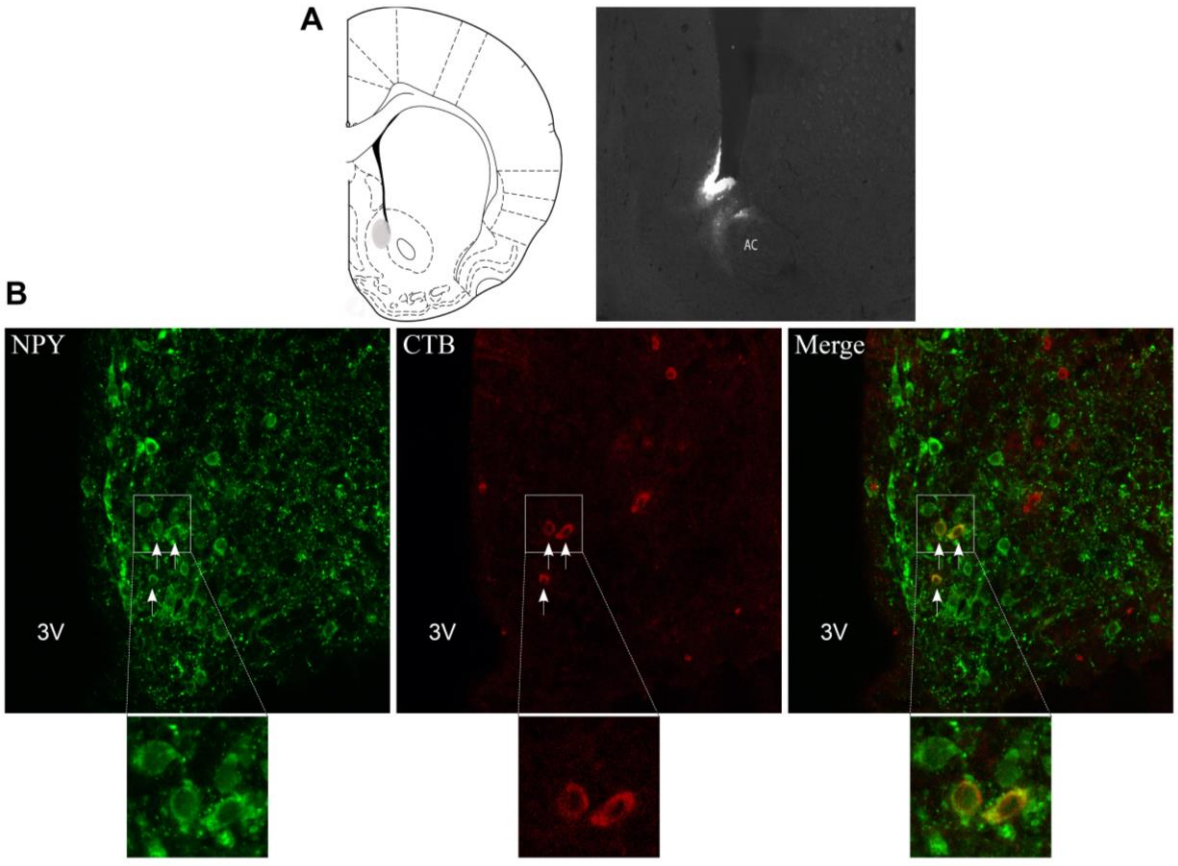

Figure 4. NPY-positive neurons in the Arc project to the NAc. A) Representative image for Cholera Toxin Beta (CTB) injection in the NAc. **B)** Confocal microscopy shows co-localization of NPY and CTB in the Arc of rats. Arrows indicate co-localization. 3V = third ventricle, AC = anterior commissure.

Discussion

In the present study, we used a combination of behavioral, neuroanatomical and *in vivo* electrophysiological measures to investigate the effect of NPY on NAc neuronal activity, neuropeptide expression and behavioral output. We demonstrated that NPY administration in the NAc in rats on a fcHFHS diet increased fat intake specifically, and this effect was attenuated by pretreatment with an NPY1R antagonist in the NAc shell. Furthermore, we identified NPY1R on ENK neurons in the NAc and found that NPY administration lowered NAc neuronal activity and levels of striatal *ppENK* mRNA. Finally, we showed that a subset of Arc NPY neurons project to the NAc. Together with our earlier findings that a fcHFHS diet increased *Npy* mRNA in the Arc and increased cerebral sensitivity for NPY (la Fleur et al., 2010; van den Heuvel et al., 2011), these findings provide evidence for a role of NPY in the intake of palatable foods, possibly via inhibition of striatal DRD_2-enkephalin neurons. Moreover, the increased levels of *Npy* mRNA in the Arc observed in rats on a fcHFHS diet may, via projections to the NAc, be related to the increased motivation and active lever pressing, as well as the persistent hyperphagia observed in these rats (la Fleur et al., 2010; la Fleur et al., 2007).

Consistent with others, we found that intra-NAc NPY did not affect chow (C. M. Brown et al., 2000; Morley, Levine, Gosnell, Kneip, & Grace, 1987), or sucrose intake (C. M. Brown et al., 2000). Interestingly, a recent study showed that intra-NAc NPY increased intake of sucrose pellets (Pandit, Luijendijk, Vanderschuren, la Fleur, & Adan, 2014b), which implies that intra-NAc NPY may increase sucrose intake in the absence of fat, or that the effect is specific to solid and not liquid sugar. NPY has been associated with carbohydrate intake in a number of studies (Morley et al., 1987; Smith et al., 1997; Stanley, Daniel, et al., 1985), yet NPY is often administered in the third ventricle or directly into hypothalamic areas. In this study, NPY was directed to the NAc and specifically increased fat intake, suggesting that the effect of NPY on food component consumption may be dependent on the specific brain region. Basal caloric intake in rats on the fcHFHS diet comprises 50% from chow, 30% from sugar and 20% from fat. Because fat is not the main preferred component under baseline conditions with this diet, we infer that NPY-induced fat intake is not confounded by a pre-existing baseline fat preference.

Our findings indicate that NPY inhibits neuronal activity in the NAc. To our knowledge, this is the first study investigating the effects of NPY on NAc neuronal activity. The inhibitory effects in the NAc are consistent with NPY's inhibitory effects in other brain areas, such as the amygdala and Arc (Acuna-Goycolea et al., 2005; Giesbrecht et al., 2010), and coincide with the downregulation of *ppENK* mRNA expression upon intra-NAc NPY administration, another novel finding in this study. This may suggest that NPY's feeding effects in the NAc may occur via downregulation of DRD_2-containing ENK neurons. The ability of NPY to reduce neuronal firing in the NAc is consistent with a general model from other pharmacological and

electrophysiological studies in which reduced NAc neuronal firing stimulates food intake (Krause et al., 2010; Sears et al., 2010). Future studies are needed to determine the precise mechanism underlying NPY's inhibitory actions in the NAc.

Mu-opioid receptor agonists (such as DAMGO) elicit robust feeding responses, however administration of different doses of Met-enkephalin or a synthetic and protease-resistant analogue of enkephalin ([D-Ala2] Met-enkephalin) in different NAc regions did not produce any significant effects on food intake (Y. Katsuura & Taha, 2010). The majority of enkephalin neurons co-express GABA (Meredith, Pennartz, & Groenewegen, 1993). Therefore, the NPY-mediated downregulation of *ppENK* neurons may also represent a reduction of GABAergic output. Reduced NAc GABAergic output has consistently been shown to elicit intense feeding in satiated rats and to increase intake of palatable foods (Basso & Kelley, 1999; Krause et al., 2010; Maldonado-Irizarry, Swanson, & Kelley, 1995; Stratford & Kelley, 1997; Stratford, Swanson, & Kelley, 1998). This reduced NAc GABAergic output likely affects food intake via the lateral hypothalamus and medial ventral pallidum (Stratford, Kelley, & Simansky, 1999). The downstream outputs from the lateral hypothalamus involve autonomic structures and structures that directly control brainstem pattern generators for the motor actions of eating (Kelley, 2004). Therefore, we speculate that the downstream mechanisms of the inhibitory effects of NPY in the NAc (leading to the increase in fat intake) involve reduced GABAergic output to the lateral hypothalamus via the medial ventral pallidum.

We demonstrated CTB tracing and NPY staining in brain areas consistent with others (Brog et al., 1993; de Quidt & Emson, 1986b). However, co-localization was only found in the Arc, suggesting that NPY neurons projecting to the NAc predominantly originate from the Arc. Although it remains to be determined whether Arc-derived NPY is the principal mediator in palatable feeding regulation when rats are on a fcHFHS diet, the NPY-ergic Arc projections to the NAc supplement findings describing α-MSH projections from the Arc to the NAc (Lim et al., 2012), and suggest that afferent signals from Arc to NAc provide input about the general metabolic state of the body. Receptors of nearly all known metabolic hormones, such as leptin, insulin, glucocorticoid and ghrelin, are present on Arc NPY neurons. It remains to be explored whether the NPY neurons that project to the NAc are also controlled by these peripheral signals.

In conclusion, our data indicate a role for NPY in the NAc in the intake of palatable food, which is likely mediated by inhibition of enkephalin neurons, probably leading to decreased GABA-ergic output. Future studies are needed to establish a direct role of GABA-ergic enkephalin neurons in NPY's effect on fat intake. Our findings confirm and extend research suggesting a role for NPY in the feeding-related neural circuit controlled by the NAc (Stratford & Wirtshafter, 2004; H. Zheng et al., 2003; H. Zheng et al., 2010). The feeding

effects of the hypothalamic peptide NPY in the NAc further links the homeostatic and hedonic feeding circuits in the control and regulation of palatable feeding.

Acknowledgements

We thank Tim Snel for helping with measuring the body weight and energy intake, and Dr. J.M. Chou-Green for English editing.

Supplemental information

A. Supplemental Methods and Materials

Surgery for cannula's in the nucleus accumbens

Male Wistar rats (Charles River, Germany) weighing 270-300 g were housed in a temperature-(21-23 °C) and light-controlled room (lights on 7:00–19:00). One week after arrival, two cannulas aimed bilaterally at the NAc shell were implanted. Rats were anaesthetized with an i.p. injection of 80 mg/kg ketamine (Eurovet Animal Health, Bladel, The Netherlands), 8 mg/kg xylazine (Bayer Health Care, Mijdrecht, The Netherlands) and 0.1 mg/kg atropine (Pharmachemie B.V., Haarlem, The Netherlands), and fixed in a stereotactic frame. Permanent 26-gauge stainless steel guide cannulas (Plastics One, Bilaney Consultants GmbH, Düsseldorf, Germany) were implanted at AP: +1.4 mm, ML: +/-2.8 mm, DV: -6.6 mm (coordinates from Bregma and using an angle of 10° in the frontal plane). Guide cannula's were secured to the skull using four anchor screws and dental cement, and occluded by a 28-gauge stainless steel dummy cannula (Plastics One, Bilaney Consultants GmbH, Düsseldorf, Germany). Immediately after surgery, rats received an analgesic subcutaneously (Carprofen, 0.5 mg/100 g body weight), and were housed individually.

Radioactive *in situ* hybridization

Sections were defrosted and fixed in 4 % paraformaldehyde (PFA) in phosphate-buffered saline (PBS) for 10 min, washed in PBS, pretreated with 0.25 % acetic anhydride in 0.1 M triethanolamine, washed again in PBS and dehydrated in graded ethanol followed by 100 % chloroform and 100 % ethanol. The sections were hybridized overnight at 72 °C with 10^6 cpm ^{33}P-labeled (33P-UTP, Perkin Elmer) antisense *ppENK* RNA probe in buffer containing 50 % deionized formamide, 2× standard saline citrate (2xSSC), 10 % dextrane sulphate, 1× Denhardt's solution, 5 mM EDTA and 10 mM phosphate buffer, after 5 min heating at 80 °C. After hybridization, the sections were washed in 5×SSC (short, 72 °C) and 0.2×SSC (2 hours, 72 °C) and dehydrated in graded ethanol in 0.3 M ammonium acetate. Sections were exposed to X-ray film (Kodak Bio-Max MR, Sigma-Aldrich, Zwijndrecht, The Netherlands) for 4 days. The films were developed and expression levels were quantitatively analyzed using an 8800F Canon scanner. All images (600 dpi) were analyzed using ImageJ (Rasband, WS, NIH, Bethesda, MD, USA, http://rsbweb.nih.gov/ij/, 1997–2005). In each section, gray values were determined in the region of interest, measured bilaterally and subtracted from background, producing a single value for each brain area on each section.

Fluorescent immunohistochemistry

Coronal slices of 35 µm were cut using a cryostat, collected, and stored until processing in cryoprotectant (30 % glycerol, 30 % ethylene glycol, 40 % 0.1 M PBS). Free-floating slices were washed in PBS at least 5 times for a total of 60 min, and were incubated in blocking buffer (2.5 % normal donkey serum, 2.5 % normal goat serum, 1 % bovine serum albumin, 1 % glycine, 1 % lysine, 0.4 % Triton X-100) for at least 30 min at room temperature (RT). Sections were incubated overnight in rabbit anti-NPY (1:1000, Niepke 091188, Netherlands Institute for Neuroscience) primary antibody diluted in blocking buffer. The next day, slices were washed in PBS several times for a total of 60 min. Subsequently, sections were incubated with donkey anti-rabbit Alexa Fluor-488 (Invitrogen) secondary antibody diluted in blocking buffer for 1 hour at RT. After 5 washes in PBS for a total of 60 min at RT, sections were mounted on glass slides, and embedded in mounting medium containing DAPI (Vectashield, Vector labs, Burlingame, CA, USA). Cholera toxin B (CTB)-Alexa-555 conjugate emission was sufficient to visualize under the fluorescent microscope without additional CTB staining. Images were first taken by fluorescent microscopy, and co-localization across all sections was determined by confocal microscope scanning.

Surgery for cannula and microwire electrode in the nucleus accumbens for neural recordings in mice

Anesthesia was initiated with ~4 % isoflurane and intraperitoneal injections of ketamine (100 mg/kg) and xylazine (10 mg/kg). A surgical level of anesthesia was maintained over the course of the surgery with supplements of ketamine (30 mg/kg) every 45–60 min. The skull was leveled between Bregma and Lambda, and a craniotomy was created over the ventral striatum. A single array of microwire electrodes was placed centered at AP: +1.2, ML: ±0.7, DV: −4.5 (coordinates from Bregma). A single infusion cannula was then placed at AP: +1.4, ML: ±2.1, DV: −4.6 (coordinates from Bregma and using an angle of 15° in the frontal plane). Craniotomies were sealed with cyanoacrylate (“Metabond”) and methyl methacrylate (i.e. dental cement; AM Systems, Carlsborg, WA, USA).

Fluorescent *in situ* hybridization

For the fluorescent *in situ* hybridization analysis, fresh frozen mouse brains were cryosectioned at 14 µm thickness and dried onto slides. The sections were then fixed in ice-cold 4 % paraformaldehyde for 20 min, dehydrated in an ethanol series, and allowed to air dry. The sections were rehydrated, acetylated for 10 min, dehydrated and air dried again. The hybridization mix (50 % formamide, 5×SSC, 5× Denhardt's solution, 250 µg/ml yeast RNA, 0.5 mg/ml salmon testes DNA, and 300 ng/ml RNA probe) was then added to the slides, which were incubated in humidified chambers at 60 °C overnight. After washing and blocking with 5 % normal rabbit IgG and 1 % blocking reagent (Roche), the NPY1R probe was first detected by

using a 1:200 anti-digoxigenin antibody coupled to HRP (Dako, Carpinteria, CA, USA). The digoxigenin signal was amplified and detected using tyramide signal amplification (TSA)-direct coupled to cyanine-3 (PerkinElmer, Wellesley, MA, USA). Hydrogen peroxide treatment (3 %, 15 min) was used to eliminate HRP activity. The fluorescein-labeled probe was detected with 1:500 rabbit anti-fluorescein coupled to HRP (Molecular Probes), followed by amplification with TSA-direct coupled to fluorescein (PerkinElmer). The sections were then dehydrated, and mounted in DPX (Fluka, Neu-Ulm, Germany).

Generation of fluorescent *in situ* hybridization probes

Amplification products obtained by PCR were gel-purified, cloned into a pCR2-TOPO vector (Invitrogen, Carlsbad, CA), and transformed into One Shot TOP10 competent cells (Invitrogen), using standard techniques. Positive clones were verified by diagnostic restriction enzyme digestion and amplicon sequencing. To generate the antisense digoxigenin (DIG)-labeled NPY1R cRNA probe, plasmids were linearized by digestion with *BAM*HI and subjected to *in vitro* transcription with T7 RNA polymerase according to the manufacturer's protocol (Roche, Basel, Switzerland). For generation of the sense DIG-labeled NPY1R cRNA probe, plasmids were linearized by digestion with *Eco*RV and subjected to *in vitro* transcription with SP6 RNA polymerase. To generate antisense fluorescein-labeled *ppENK* and *pDYN* cRNA probes, plasmids were linearized by digestion with *BAM*HI for *ppENK* and *Eco*RV for *pDYN*, and subjected to *in vitro* transcription with T7 RNA polymerase (for *ppENK*), or SP6 (for *pDYN*) according to the manufacturer's protocol (Molecular Probes, Eugene, OR, USA). Hybridization with sense probes was included as a control to confirm the specificity of the *in situ* hybridization protocol. These sense hybridization probes did not show any fluorescent hybridization signal.

Table S1. *In situ* hybridization primers.

	NCBI reference number	Primers	Product size	Transcript nucleotide number
Npy1r	NM_010934	Forward: GAAGCAGGCTAGCCCAGTC Reverse: TCAGGTGGTGACTGCTTTTG	506	1337-1882
ppENK	NM_001002927	Forward: AACAGGATGAGAGCCACTTG Reverse: CTTCATCCGAGGGTAGAGAC	437	568-1041
pDYN	NM_018863	Forward: TCTTTTCTCACCCTGACTGC Reverse: CCATAGCGTTTGTACAGGTC	371	510-916

Npy1r = Neuropeptide Y receptor subtype 1, *pDyn* = prodynorphin, *ppENK* = preproenkephalin

B. Supplemental Results

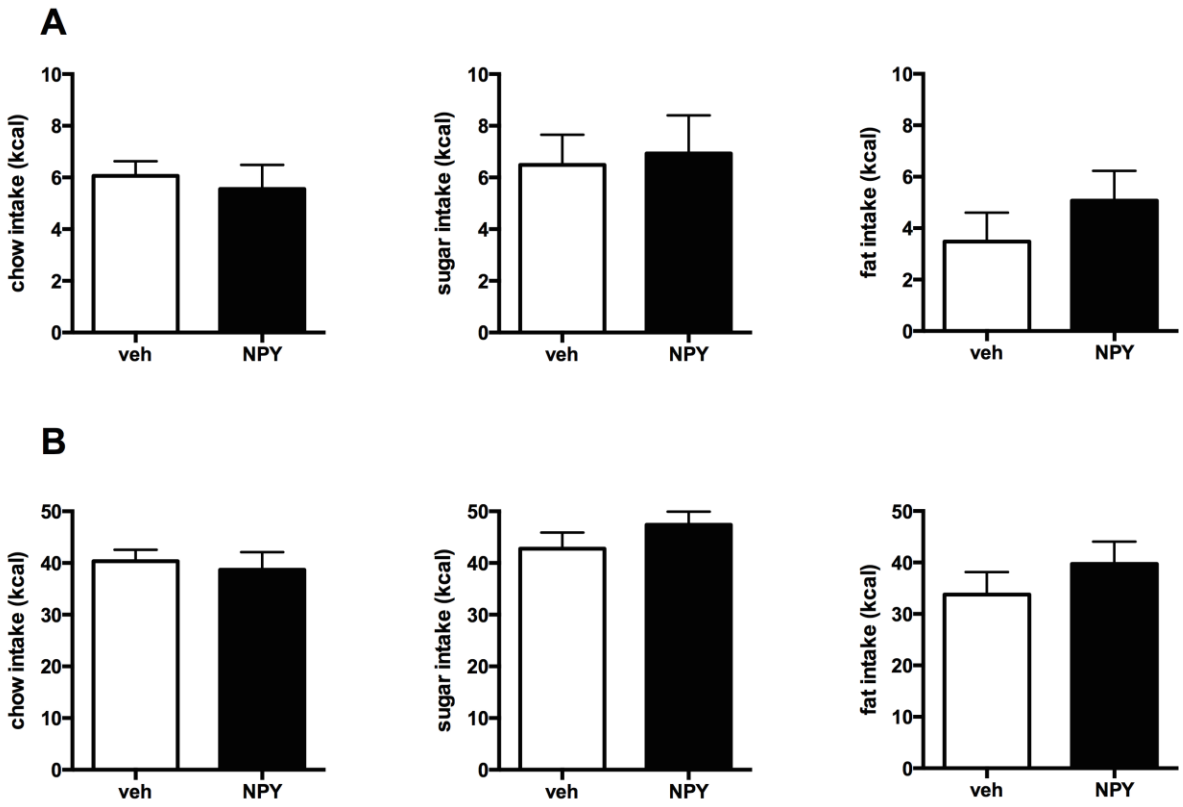

Figure S1. Effect of intra-NAc NPY on **A)** 5-hour, and **B)** 24-hour intake of the chow, sugar (sucrose water), and fat component. The intake of chow, sugar (sucrose water), and fat is not increased after 5 or 24 hours after NPY administration in the NAc of male Wistar rats. NAc = nucleus accumbens, NPY = Neuropeptide Y, veh = saline vehicle.

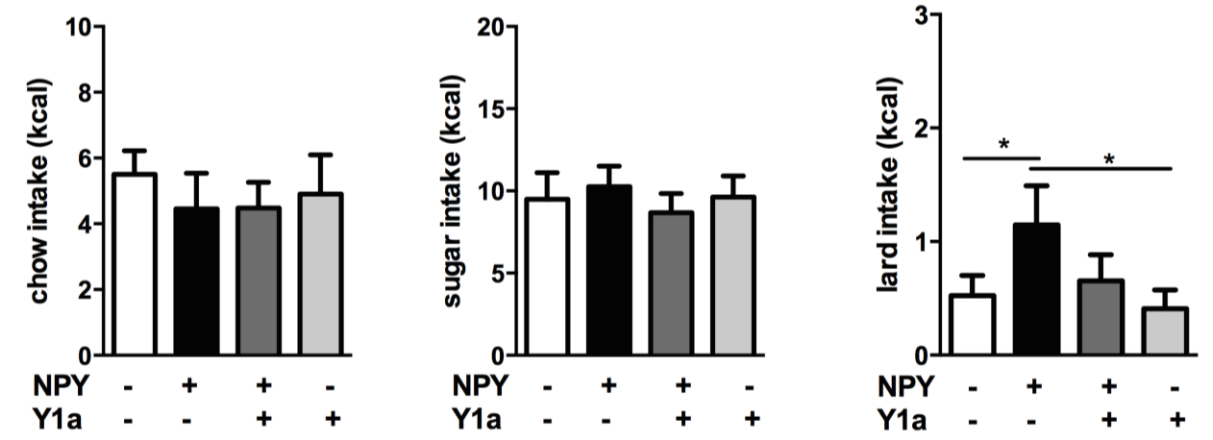

Figure S2. Effect of pretreatment with NPY receptor subtype 1 antagonist (Y1a) on NPY-induced fat intake in rats with uni- or bilateral cannula placement in the NAc shell (N = 11). Rats with unilateral or bilateral cannula placement in the Nac shell showed increased fat intake, consistent with Figure 1A. Pretreatment with the NPY1R antagonist GR231118 (Y1a) did not significantly attenuate the NPY-induced fat intake (Figure 1B; Two-way repeated measures ANOVA: effect of NPY $F_{1,10} = 4.6$; $p = 0.06$; effect of pretreatment $F_{1,10} = 5.3$; $p = 0.04$), but no interaction effect of NPY* pretreatment ($F_{1,10} = 1.0$; $p = 0.34$); post hoc: *$p < 0.05$. Interestingly, only when the NPY1R antagonist was infused bilaterally in the medial shell, were NPY's effects on fat intake completely abolished, suggesting an important role of the medial shell in the NPY1R mediated effects, and that the NPY1R in the NAc-shell is involved in the effect of NPY on fat intake. NAc = nucleus accumbens, NPY = Neuropeptide Y.

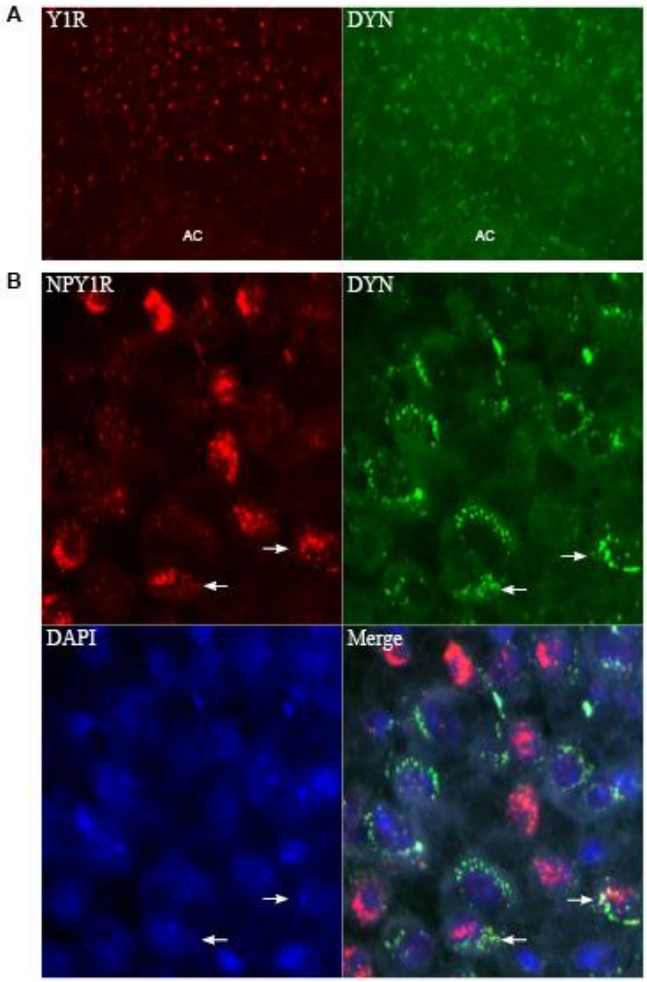

Figure S3. A) Fluorescent microscopy shows the expression pattern of *dynorphin* (DYN) and *NPY receptor subtype 1* (Y1R) mRNA in the nucleus accumbens (NAc). **B**) Confocal microscopy showing co-localization of *Npy1r* on a subpopulation of *DYN* neurons in the NAc. Horizontal arrows indicate co-localization. AC = anterior commissure, DAPI = nuclear staining.